Inorganic Chemistry

pubs.acs.org/IC

Article

Reductive C−O Cleavage of Ethereal Solvents and 18-Crown-6 in $Ln(NR_2)_3/KC_8$ Reactions ($R = SiMe_3$)

Amanda B. Chung,[#] Cary R. Stennett,[#] William N. G. Moore, Ming Fang, Joseph W. Ziller, and William J. Evans*

Cite This: Inorg. Chem. 2023, 62, 5854−5862

Read Online

ACCESS | Metrics & More | Article Recommendations | Supporting Information

ABSTRACT: The high reactivity accessible from the reduction of the tris(amide) complexes $Ln(NR_2)_3$ ($R = SiMe_3$) with potassium graphite in the presence of a variety of ethers is demonstrated by crystal structures of six different types of products of C−O bond cleavage reactions with Ln = Y, Ho, Er, and Lu. Specifically, 1,2-dimethoxyethane (DME) can be cleaved in $Ln(NR_2)_3/KC_8$ reactions as shown by three different types of crystals: $[K(crypt)][(R_2N)_3Y(OCH_2CH_2OCH_3)]$, **1-Y**, $[(R_2N)_2Y(\mu\text{-}OCH_2CH_2OCH_3\text{-}\kappa O,\kappa O')]_2$, **2-Y**, and $[K_2(18\text{-c-}6)_3]\{[(R_2N)_3Lu]_2[(\mu\text{-}OCH_2CH_2O)]\}$, **3-Lu** (18-c-6 = 18-crown-6; crypt = 2.2.2-cryptand). THF can be ring opened by the $Y(NR_2)_3/KC_8$ reaction system, as shown by crystals of the butoxide, $[K(crypt)][(R_2N)_3Y(OCH_2CH_2CH_2CH_3)]$, **4-Y**. The cyclic ether, oxetane, OC_3H_6, ring opens in $Ln(NR_2)_3/KC_8$ reactions to form crystals of the propoxide, $[K(18\text{-c-}6)(OC_3H_6)][(R_2N)_3Ln(OCH_2CH_2CH_3)]$, **5-Ln**, for Ln = Ho and Er. In Et_2O, the $Y(NR_2)_3/KC_8$ reactions do not attack the solvent, but C−O cleavage of 18-c-6 is observed to form $\{[(R_2N)_2]Y[\mu\text{-}\eta^1\text{:}\eta^1\text{-}O_2(C_{10}H_{20}O_4)K]\}_2$, **6-Y**. These $Ln(NR_2)_3/KC_8$ C−O cleavage reactions are typically accompanied by C−H bond activation reactions, which form cyclometalates such as $[K(crypt)]\{(R_2N)_2Ln[N(SiMe_3)(SiMe_2CH_2)\text{-}\kappa C,\kappa N]\}$, **7-Ln** (Ln = Y, Ho, Er), and $[K(18\text{-c-}6)]\{(R_2N)_2Y[N(SiMe_3)(SiMe_2CH_2)\text{-}\kappa C,\kappa N]\}$, **8-Y**, which are common decomposition products of $Ln(NR_2)_3$ reactions. In addition, in this study, the hydride complex, $[K(18\text{-c-}6)][(R_2N)_3YH]$, **9-Y**, was isolated. NMR analysis indicates that the yttrium reactions form mixtures that consistently contain the yttrium cyclometalates **7-Y** and **8-Y** as major components. These results show the diversity of available reaction pathways for the $Ln(NR_2)_3/KC_8$ system and highlight the inherent difficulties in isolating Ln(II) complexes containing the $[Ln(NR_2)_3]^{1-}$ anion.

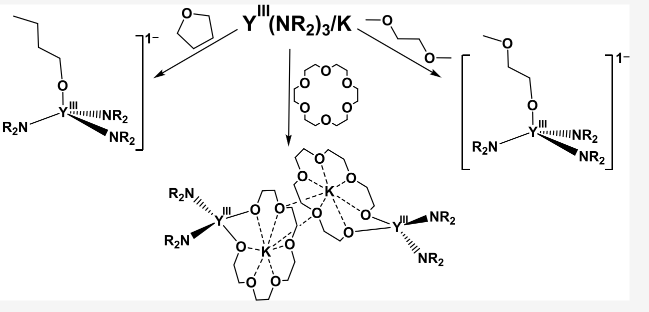

■ INTRODUCTION

Among the many seminal studies of the late Professor Michael F. Lappert were attempts to synthesize molecular complexes of rare-earth metals in the +2 oxidation state[1−9] beyond the known examples with the traditional Ln(II) ions, namely, Eu(II), Yb(II), Sm(II), Tm(II), Dy(II), and Nd(II).[10−14] Lappert's initial studies of the reduction of tris(cyclopentadienyl) rare-earth metal complexes with potassium or lithium in 1,2-dimethoxyethane (DME) led to cleavage of the solvent and formation of methoxide complexes (eq 1).[1]

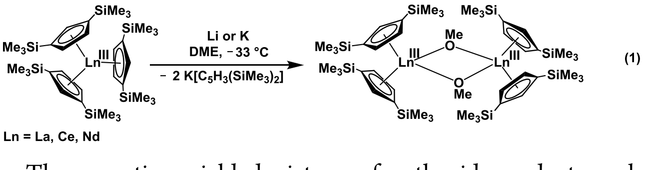

(1)

These reactions yielded mixtures of methoxide products, such as $[Cp''_2\ Ln(\mu\text{-}OMe)]_2$ [Ln = La,[3] Ce,[1] and Nd;[3] $Cp'' = C_5H_3(SiMe_3)_2$], eq 1, and $[Cp''_2Nd(\mu\text{-}OMe)_2Li(DME)]$,[1] along with KCp″ and unidentified polymetallic methoxide complexes. These results were consistent with earlier predictions that any Ln(II) ion beyond Eu, Yb, Sm, Tm, Dy, and Nd would be so reducing that they would decompose any solvent in which they were soluble.[11,13−15]

However, when Lappert switched to THF and Et_2O solvents in the presence of 18-crown-6 (18-c-6) and 2.2.2-cryptand (crypt), La(II) and Ce(II) complexes could be identified (eq 2).[8] Subsequently, using $(C_5H_4SiMe_3)_3Ln$, precursors, Ln(II) complexes were isolated for the whole lanthanide series in THF (eq 2).[16]

Received: March 1, 2023
Published: March 29, 2023

https://doi.org/10.1021/acs.inorgchem.3c00689
Inorg. Chem. 2023, 62, 5854−5862

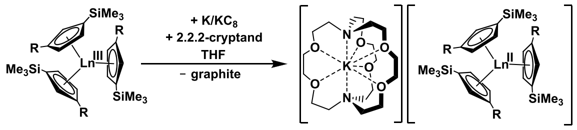

(2)

R = SiMe$_3$; Ln = La, Ce, Pr, Nd

R = H; Ln = La, Ce, Pr, Nd, Sm, Gd, Tb, Dy, Ho, Er, Tm, Yb, Lu, Y

The reactivity of isolated $(Cp''_3Ln^{II})^{1-}$ complexes with DME was subsequently investigated, and it was found that the isolated Ln(II) complexes slowly react with DME but do not form the methoxide complexes of eq 1 generated by in situ Cp''_3Ln/K reactions.[17] This was one of several examples of the difference in reactivity of isolated Ln(II) complexes, $[Ln^{II}A_3]^{1-}$ (A = anion) versus in situ $Ln^{III}A_3$/M reactions (M = alkali metal).[18−20]

Subsequent studies of the reduction of $Cp^{Me}{}_3Ln$ (Cp^{Me} = C_5H_4Me) in THF revealed another way in which in situ LnA_3/M reactions can decompose solvents. For Ln = La and Pr, this led to ring opening of THF to form the $(OCH_2CH_2CH_2CH_2)^{2-}$ dianion (eq 3).[21]

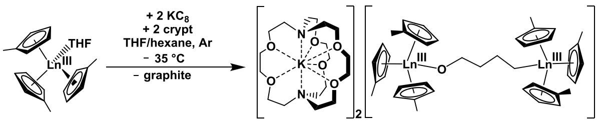

(3)

Ln = La, Pr

Although solvent decomposition by $Cp^x{}_3Ln$/K (Cp^x = Cp″, Cp^{Me}) reactions has been described in several cyclopentadienyl systems, little information is available on the amide reaction manifold, $Ln(NR_2)_3$/K. Here, we provide more information on solvent reactivity in these reductive amide systems by describing a series of C−O cleavage products isolated from $Ln(NR_2)_3$/K reactions (R = $SiMe_3$). Thus, this study expands solvent reactivity reactions to reductions with ligands beyond cyclopentadienyls. It also provides more examples of the high reactivity obtainable by the LnA_3/M combinations in solution before crystalline Ln(II) complexes are isolated. This emphasizes the need to run these reduction reactions quickly and minimize the time the Ln(II) products are in solution.

The products reported here were obtained in reduction reactions that quickly lost the characteristic dark color of Ln(II) ions in solution. The C−O cleavage products were isolated in low yield and were likely obtained, not necessarily because they were the main reaction product, but rather because they were the least soluble and most crystallizable. Although these are not the major products of these reactions, they constitute a warning of possible routes by which reductive rare-earth reactions can be altered by solvent reactivity and by which Ln(II) complexes can decompose in solution. NMR studies on the yttrium reactions typically showed the presence of the ligand-metalated anion, $\{(R_2N)_2Y[N(SiMe_3)(SiMe_2CH_2)\text{-}\kappa C,\kappa N]\}^{1-}$, as a major component of the complicated product mixture. This is not unusual since these cyclometalated anions are common decomposition products in $Ln(NR_2)_3$ reactions[22,23,32−40,24−31] and a salt of this anion, $[K(18\text{-crown-6})(THF)(toluene)]\{(R_2N)_2Ln[N(SiMe_3)(SiMe_2CH_2)\text{-}\kappa C,\kappa N]\}$, was crystallized from a $Ln(NR_2)_3$/K reaction long ago.[23]

■ RESULTS AND DISCUSSION

Dimethoxyethane (DME). The addition of a chilled DME solution (−35 °C) of $Y(NR_2)_3$ (R = $SiMe_3$) and 2.2.2-cryptand (crypt) to a −35 °C-chilled vial of excess solid KC_8 produced a dark blue solution that quickly becomes light yellow. After removal of spent KC_8 by filtration and crystallization under hexanes, colorless crystals form, which were identified by X-ray crystallography as $[K(crypt)][(R_2N)_3Y(OCH_2CH_2OCH_3)]$, **1-Y** (Figure 1, eq 4).

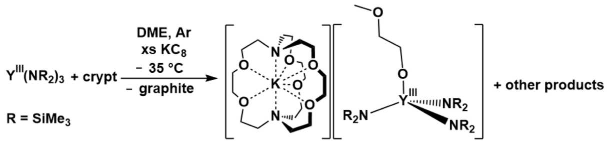

(4)

1-Y

Complex **1-Y** is evidently formed by the cleavage of a Me−O bond of a DME molecule and differs from the DME cleavage products in eq 1 that involved cleavage of an O−CH_2 linkage. Analogous reactions in DME using 18-crown-6 (18-c-6) instead of crypt also displayed dark-blue to light-yellow color transitions, but the crystal structures of these products could not be solved.

In one $Y(NR_2)_3/KC_8$ reaction in the absence of crypt or 18-c-6, a neutral bimetallic DME decomposition product was isolated, $[(R_2N)_2Y(\mu\text{-}OCH_2CH_2OMe\text{-}\kappa O,\kappa O')]_2$, **2-Y** (Figure 2, eq 5).

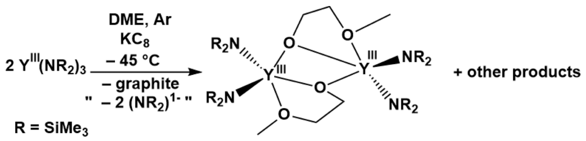

(5)

2-Y

As in the formation of **1-Y**, complex **2-Y** results from cleavage of a C−O bond that excises a methyl group from DME. However, in this case the methoxyethoxide ligand bridges two yttrium centers with the anionic oxygen donor atom and chelates to one of the yttrium centers with the ether oxygen. The fate of the methyl group in this reaction is unknown.

The formation of **2-Y** involves a net loss of one $(NR_2)^{1-}$ ligand per metal. The isolation of a neutral complex with two amides per metal in this C−O cleavage reaction instead of an anionic complex with three amides per metal may be related to the fact that no potassium chelate was present to help stabilize the countercation as occurred in **1-Y**. The loss of one amide ligand per metal is compensated in the coordination environment by the bridging and chelating nature of the methoxyethoxide ligand. Loss of amide ligands in $Ln(NR_2)_3$/K reactions is common, e.g., in the reduction of N_2, which generates the $[(R_2N)_2(THF)Ln]_2N_2$ products with two amides per metal. In addition, $KLn(NR_2)_4$ byproducts are sometimes isolated in these reactions and are presumably formed from addition of KNR_2

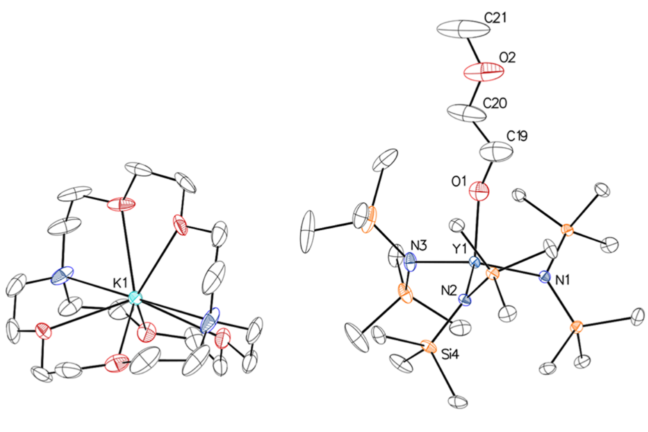

Figure 1. The molecular structure of $[K(crypt)][(R_2N)_3Y(OCH_2CH_2OCH_3)]$, **1-Y**, with thermal ellipsoids drawn at the 50% probability level. For clarity, hydrogen atoms are not shown.

https://doi.org/10.1021/acs.inorgchem.3c00689
Inorg. Chem. 2023, 62, 5854−5862

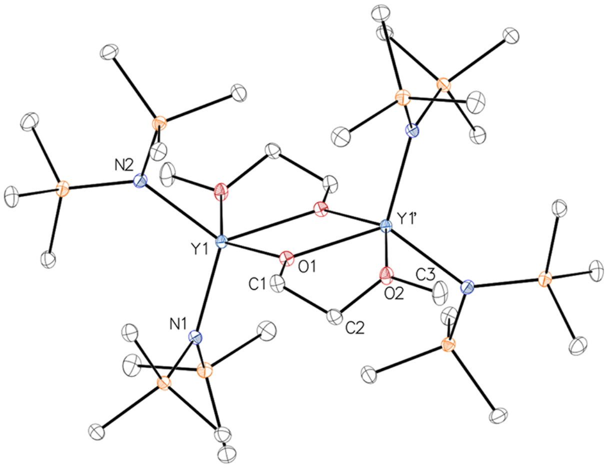

Figure 2. The molecular structure of $[(R_2N)_2Y(\mu\text{-}OCH_2CH_2OMe\text{-}\kappa O,\kappa O')]_2$, **2-Y**, with thermal ellipsoids drawn at the 30% probability level. For clarity, hydrogen atoms are not shown.

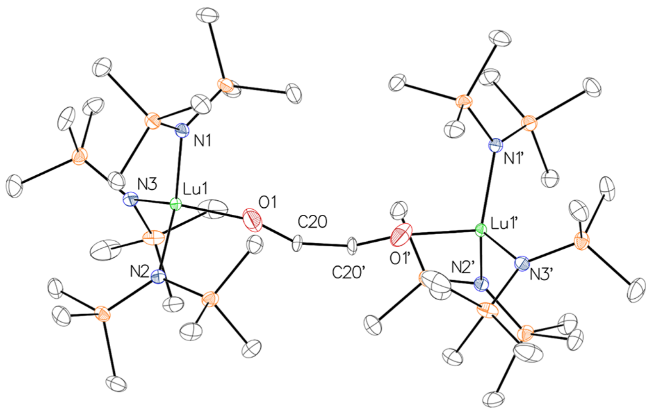

Figure 3. The molecular structure of $[K_2(18\text{-c-}6)_3]\{[(R_2N)_3Lu]_2[(\mu\text{-}OCH_2CH_2O)]\}$, **3-Lu**, with thermal ellipsoids drawn at the 30% probability level. For clarity, hydrogen atoms, $[K_2(18\text{-c-}6)_3]^{2+}$, a molecule of Et_2O, and a molecule of hexanes are not shown.

to the $Ln(NR_2)_3$ starting material.[41] If the amide ligand is lost as KNR_2, it can explain the presence of the cyclometalated product, $\{(R_2N)_2Y[N(SiMe_3)(SiMe_2CH_2)\text{-}\kappa C,\kappa N]\}^{1-}$, described below in the NMR studies, since KNR_2 readily reacts with $Y(NR_2)_3$ to form this cyclometalate.

Complex **1-Y** can also be generated by adding DME to a preformed solution of $[Y(NR_2)_3]^{1-}$ in Et_2O. Specifically, addition of a −35 °C-chilled Et_2O solution of $Y(NR_2)_3$ and crypt to excess chilled KC_8 generated a dark-blue solution characteristic of the Y(II) ion.[18] After filtration to remove graphite and unreacted KC_8, addition of a stoichiometric or excess amount of DME, chilled to −35 °C, immediately turned the solution light-yellow. Recrystallization by layering this solution beneath hexanes at −35 °C produced colorless crystals of **1-Y**, which were crystallographically characterized.

$Ln(NR_2)_3/KC_8$ reactions in DME in the presence of crypt and 18-c-6 were also examined with three lanthanide metals similar in size to yttrium, namely, Ln = Ho, Er, and Lu.[42] In all cases, reduction of the $Ln(NR_2)_3$ complexes in DME solutions at −35 °C using excess cold KC_8 in the presence of either crypt or 18-c-6 produced dark-blue solutions that immediately turn to light yellow. Only the reaction of $Lu(NR_2)_3$ with KC_8 in the presence of 18-c-6 gave a crystallographically characterizable product. After removal of spent KC_8 by filtration and layering of the solution under hexanes, colorless crystals form, which were identified by X-ray crystallography as $[K_2(18\text{-c-}6)_3]\{[(R_2N)_3Lu]_2[(\mu\text{-}OCH_2CH_2O)]\}$, **3-Lu** (Figure 3, eq 6).

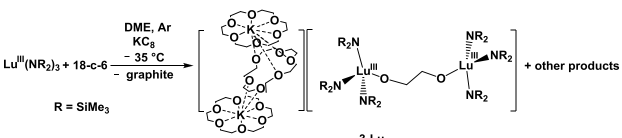

(6)

3-Lu

Like **1-Y** and **2-Y**, this product is formed by cleavage of Me−O bonds, but in this case, both of the Me−O bonds of a DME molecule were cleaved and the resulting $(OCH_2CH_2O)^{2-}$ dianion was trapped between two lutetium centers. The isolation of **3-Lu** containing a dianionic DME cleavage fragment may be facilitated by the presence of 18-crown-6 instead of crypt, since it can form the dicationic $[K_2(18\text{-c-}6)_3]^{2+}$ countercation.

To better understand the nature of the decomposition of $[Y\{N(SiMe_3)_2\}_3]^{1-}$ under these conditions, a ^1H NMR study of the $Y\{N(SiMe_3)_2\}_3/KC_8$/crypt reaction in DME solvent was conducted. The spectrum of the previously reported cyclometalated $\{(R_2N)_2Y[N(SiMe_3)(SiMe_2CH_2)\text{-}\kappa C,\kappa N]\}^{1-}$ anion[23] was observed as well as a set of signals with a 2:2:3:54 integration ratio and multiplicities consistent with the presence of the $[(R_2N)_3Y(OCH_2CH_2OCH_3)]^{1-}$ anion in **1-Y** (see the SI). The ratio of intensities of the cyclometalate and the anion in **1-Y** was approximately 16:9. Based on the mass of the solids obtained from this solution, the estimated yields were 31 and 17%, respectively, if there were no other products in solution. Additional resonances were observed in the NMR spectrum that cannot be correlated with a known compound, so these are maximum yields. This included two additional resonances in the $SiMe_3$ region and a low intensity doublet at −0.61 ppm (J = 2.5 Hz) consistent with the presence of another complex containing a Y-CH_2 moiety. Similar results to these were obtained when the same reaction was performed using 18-crown-6 as the chelate. Again, an approximate 16:9 ratio of the cyclometalate to the anion in **1-Y** was observed. In this case, the yields were 25 and 14% based on the amount of solid material isolated and if no other products were in solution.

Tetrahydrofuran (THF). The reduction of a −35 °C solution of $Y(NR_2)_3$ in THF with excess KC_8 in the presence of crypt also produced a dark-blue solution as is observed when DME is used as the solvent. After the spent KC_8 is removed by filtration, the dark-blue solution remained colored at −35 °C for about an hour before it turned yellow. Layering of this solution beneath hexanes and storage at −35 °C yielded colorless crystals, which were identified by X-ray crystallography as the butoxide complex $[K(crypt)][(R_2N)_3Y(OCH_2CH_2CH_2CH_3)]$, **4-Y** (eq 7, Figure 4). Complex **4-Y** is apparently formed by ring opening of the THF solvent. Formation of n-butoxide complexes by nucleophilic hydride attack on THF that has been activated by a Lewis acidic metal has been reported for many metals,[43−51] although THF decomposition with formation of

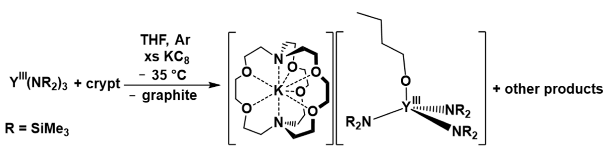

(7)

4-Y

https://doi.org/10.1021/acs.inorgchem.3c00689
Inorg. Chem. 2023, 62, 5854−5862

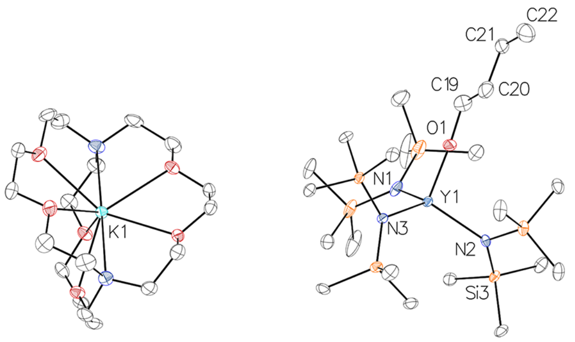

Figure 4. The molecular structure of $[K(crypt)][(R_2N)_3Y(OCH_2CH_2CH_2CH_3)]$, **4-Y**. Thermal ellipsoids are drawn at the 30% probability level. For clarity, hydrogen atoms are not shown.

$(OCH{=}CH_2)^{1-}$ complexes is also quite common.[52−56] THF decomposition products containing $(OCH_2CH_2CH{=}CH_2)^{1-}$[57] and O^{2-}[58−60] have also been reported as well as complexes of the $(OCH_2CH_2CH_2CH_2)^{2-}$ dianion in eq 3. The presence of hydride ligands in this system arising from ligand metalation is discussed below.

A ^1H NMR study of the $Y\{N(SiMe_3)_2\}_3/KC_8$/crypt reaction in THF solvent again showed the formation of the cyclometalate anion, $\{(R_2N)_2Y[N(SiMe_3)(SiMe_2CH_2)\text{-}\kappa C,\kappa N]\}^{1-}$. Additional signals were found in a 2:2:2:3:54 ratio, which had multiplicities consistent with the $[(R_2N)_3Y(OCH_2CH_2CH_2CH_3)]^{1-}$ anion of **4-Y**. The intensities indicated that the cyclometalate and butoxide were formed in an approximate 1:1 ratio. The presence of an additional singlet resonance at −0.21 ppm corresponding to a complex, which has not yet been identified, precluded the determination of the yields of the cyclometalate and the butoxide. When the analogous reaction with 18-c-6 as the chelate was examined, i.e., $Y\{N(SiMe_3)_2\}_3/KC_8$/18-c-6 in THF, an approximate 4:1 ratio of the cyclometalate to the butoxide was observed with estimated maximum yields of 46 and 12%, respectively.

The $Y\{N(SiMe_3)_2\}_3/KC_8$/18-c-6 reaction was also performed in THF-D_8 and examined by NMR spectroscopy. Resonances for the cyclometalate, $\{(R_2N)_2Y[N(SiMe_3)(SiMe_2CH_2)\text{-}\kappa C,\kappa N]\}^{1-}$, were observed in the ^1H NMR spectrum, as well as a singlet resonance corresponding to the protons of the $-N(SiMe_3)_2$ ligands of the butoxide complex **4-Y**. An additional resonance at −0.21 ppm was observed that cannot be identified. The ^2H NMR spectrum of the same sample (Figure 5), showed four resonances corresponding to the deuterons of the butoxide ligand of **4-Y**. Additionally, H−D coupling (J_{HD} = 1.9 Hz)[61] was observed in the 0.87 ppm resonance corresponding to the methyl group of the deuterated butoxide ligand, indicating that the H atom in this position does not originate from the solvent since it would be deuterium in this THF-D_8 reaction. If the source of the hydrogen in this position is the deprotonation of a methyl group of a $-N(SiMe_3)_2$ ligand, this would explain the formation of both the butoxide complex **4-Y** and the cyclometalate.

Oxetane, C_3H_6O. Ring opening of the cyclic ether, oxetane, was also examined. When dark-blue solutions of $[Ln^{II}(NR_2)_3]^{1-}$, generated by reduction of chilled Et_2O solutions of $Ln(NR_2)_3$ and 18-c-6 with chilled excess KC_8, were treated with oxetane and swirled, they turned yellow. No crystallographically characterizable products were isolated for Ln = Y, but for Ln = Ho and Er, the ring-opened oxetane complex $[K(18\text{-}c\text{-}6)(OC_3H_6)][(R_2N)_3Ln(OCH_2CH_2CH_3)]$, **5-Ln** (Ln = Ho, Er)

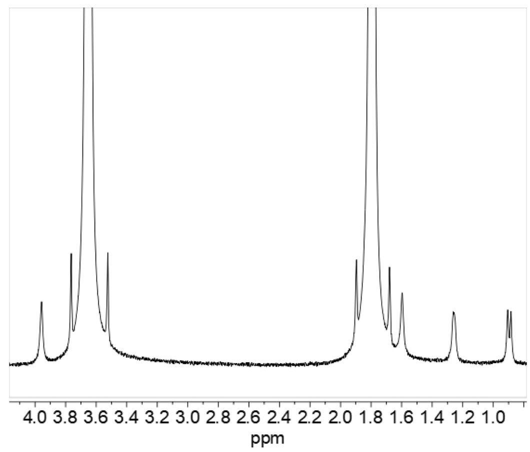

Figure 5. Magnified ^2H NMR spectrum (92 MHz, THF) of $[K(18\text{-}c\text{-}6)][(R_2N)_3Y(OCD_2CD_2CD_2CD_2H)]$, **4-Y**, showing the H−D coupling resulting from the CD_2H moiety of the butoxide ligand. The intense signals (and associated satellite signals) at ca. 3.7 and 1.8 ppm are due to residual THF-D_8.

(eq 8, Figure 6), can be isolated (see the SI for Ln = Er). This reaction is similar to that in eq 7 in which the ether is ring opened to make an alkoxide, in this case, *n*-propoxide.

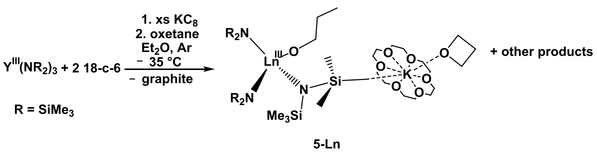

(8)

Interestingly, an intact oxetane is also found in the crystal structure coordinating to the potassium 18-c-6 moiety. The X-ray crystal structure shows a methyl group of an $(NR_2)^{1-}$ ligand oriented toward the potassium in the crown in the side opposite the coordinated oxetane. This type of structure has been observed before with the $[K(18\text{-}c\text{-}6)]^{1+}$ cation.[62−66]

18-Crown-6. Previously, low-temperature reductions of $Y(NR_2)_3$ with excess KC_8 in Et_2O allowed isolation of the Y(II) complex, $[K(18\text{-}c\text{-}6)_2][Y(NR_2)_3]$.[18] This complex can be crystallographically characterized, although it decomposes in solution in less than 5 h at −35 °C.[18] In one case in a reaction exploring CO activation, a C−O cleavage decomposition product was crystallizable. However, the product was not the result of Et_2O solvent cleavage, but instead decomposition of the

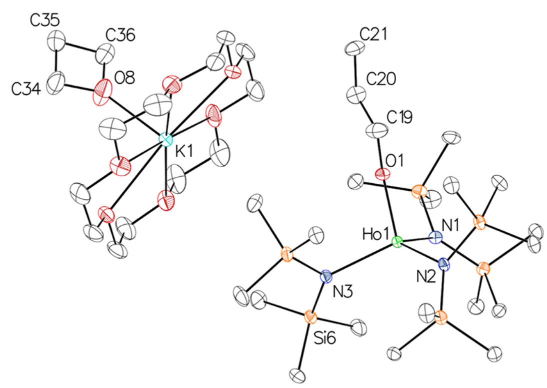

Figure 6. The molecular structure of $[K(18\text{-}c\text{-}6)(OC_3H_6)][(R_2N)_3Ho(OCH_2CH_2CH_3)]$, **5-Ho**, with atomic displacement parameters drawn at the 50% probability level. Hydrogen atoms are excluded for clarity.

https://doi.org/10.1021/acs.inorgchem.3c00689
Inorg. Chem. 2023, 62, 5854−5862

18-c-6 chelate, $\{[(R_2N)_2]Y[\mu\text{-}O_2(C_{10}H_{20}O_4\text{-}\kappa O,\kappa O')K]\}_2$, **6-Y** (eq 9, Figure 7). This product arises from two O−CH_2 cleavage reactions in the ring of an 18-c-6 molecule that formally eliminate an ethylene unit.

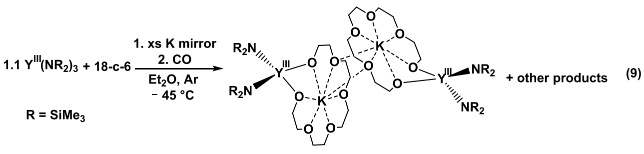

6-Y

This generates a cyclic bis(alkoxide) dianion complex, which has a potassium atom in the center of the cleaved crown ether and the yttrium center chelated by the two alkoxide functionalities. Previously, the formal loss of ethylene from crypt has been observed in an attempt to synthesize Sm(I) complexes by reduction of $[C_5H_3(SiMe_3)_2]_2Sm(THF)$.[67] Complex **6-Y** crystallizes as a dimer with two of the 18-crown-6 derived bis(alkoxide) units connected with K−O′ and K′−O linkages. $[K(18\text{-crown-6})]^{1+}$ units are known to dimerize,[68−72] so this aspect of the structure is precedented.

Formation of Cyclometalated Decomposition Products. As described above in the NMR studies, in addition to the C−O bond cleavage products isolated from the reductions of amide-ligated rare-earth metal complexes in this study, products of C−H bond activation were also identified. In the $Y(NR_2)_3$/KC_8 reaction system in Et_2O in the presence of crypt, the complex $[K(crypt)]\{(R_2N)_2Y[N(SiMe_3)(SiMe_2CH_2)\text{-}\kappa C,\kappa N]\}$, **7-Y**, can be isolated and crystallographically characterized (eq 10, Figure 8). The anion in **7-Y** was previously reported as the $[K(C_6H_6)_2]^{1+}$ salt from the reaction of $Y[N(SiMe_3)_2]_3$ with $KSi(SiMe_3)_3$[22] and as the $[K(18\text{-c-}6)(THF)(toluene)]^{1+}$ salt from the $Y(NR_2)_3/KC_8$ reaction in THF at room temperature.[23]

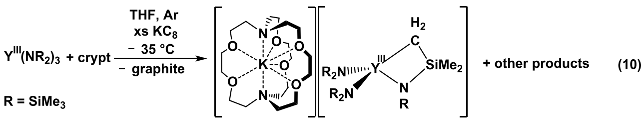

7-Y

The $[N(SiMe_3)_2]^{1-}$ ligand is well known to form cyclometalated products containing the $[N(SiMe_3)(SiMe_2CH_2)\text{-}\kappa C,\kappa N]^{2-}$ dianion.[22−30] Furthermore, the formation of this dianion by C−H bond activation has also been specifically found in numerous reduction reactions involving rare-earth and actinide metals.[9,24,29−40,73−75] Complex **7-Y** was also isolated from the −35 °C reduction of $Y(NR_2)_3$ with excess KC_8 in the presence of crypt in a 1:1 solution of DME:THF that was carried out to explore whether Y(II) would preferentially react with THF or DME. As in the other reactions, the dark-blue Y(II) solution quickly turned to light yellow. However, in this case, the only decomposition product that was identified crystallographically is **7-Y**.

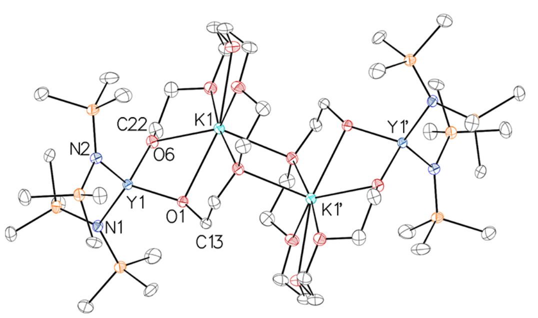

Figure 7. The molecular structure of $\{[(R_2N)_2]Y[\mu\text{-}O_2(C_{10}H_{20}O_4-\kappa O,\kappa O')K]\}_2$, **6-Y**, drawn at the 30% probability level. For clarity, hydrogen atoms are not shown.

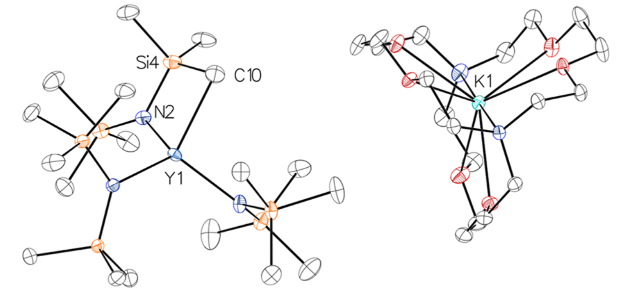

Figure 8. The molecular structure of the anion $[K(crypt)]\{(R_2N)_2Y\text{-}[N(SiMe_3)(SiMe_2CH_2)\text{-}\kappa C,\kappa N]\}$, **7-Y**, with atomic displacement parameters drawn at the 50% probability level. For clarity, hydrogen atoms and minor (25%) positional disorder of the Y atom are not shown.

To obtain more data on this THF versus DME competition, the reaction mixture was examined by ^1H NMR spectroscopy. NMR resonances for the cyclometalate anion in **7-Y**, the butoxide anion in **4-Y**, and the methoxyethoxide anion in **1-Y** can all be observed. Again, cyclometalate was the main product in the reaction and the intensities had an approximate ratio of 11:8:1, for the anions of **7-Y**, **4-Y**, and **1-Y**, respectively. It is interesting that more of the THF cleavage product is observed compared to the DME product since DME has traditionally been more commonly found to decompose in these reduction reactions.[1,17]

Coincidentally, the structure of complex **7-Y** is isomorphous with the structures of the Ln(II) complexes, $[K(crypt)]\text{-}[(R_2N)_3Ln]$, **10-Ln**, for Ln = Gd, Tb, Dy, Sc.[76] This has previously been observed for other pairs of complexes involving $[N(SiMe_3)_2]^{1-}$ and $[N(SiMe_3)(SiMe_2CH_2)\text{-}\kappa C,\kappa N]^{2-}$, e.g., $[K(crypt)][(C_5Me_5)_2Y\{N(SiMe_3)(SiMe_2CH_2)\text{-}\kappa C,\kappa N\}]$ and $[K(crypt)][(C_5Me_5)_2Y(NR_2)]$ and $[K(crypt)][(C_5Me_4H)_2Y\text{-}\{N(SiMe_3)(SiMe_2CH_2)\text{-}\kappa C,\kappa N\}]$ and $[K(crypt)]\text{-}[(C_5Me_4H)_2Y(NR_2)]$.[29] Comparison of **7-Y** with **10-Y** for yttrium is not possible since **10-Y** has not been crystallographically characterized. However, the holmium and erbium cyclometalates, $[K(crypt)]\{(R_2N)_2Ln[N(SiMe_3)(SiMe_2CH_2)\text{-}\kappa C,\kappa N]\}$, **7-Ln** (Ln = Ho, Er), can be isolated from the reduction of $Ln(NR_2)_3$ with excess KC_8 in the presence of crypt in Et_2O, and they too are isomorphous with **10-Ln** and the other structures (see the SI).

When 18-crown-6 was used instead of crypt in the analogous reaction of $Y(NR_2)_3$ with excess KC_8 in Et_2O, the same anion was isolated with a different countercation, $\{[K(18\text{-c-}6)]\text{-}\{(R_2N)_2Y[N(SiMe_3)(SiMe_2CH_2)\text{-}\kappa C,\kappa N]\}\}_n$, **8-Y** (eq 11, Figure 9).

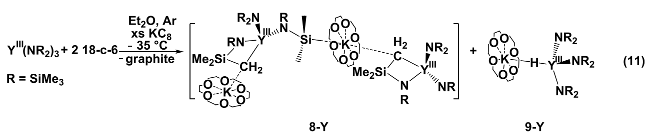

8-Y **9-Y**

\+ other products

In this case, the complex crystallized as an extended structure in which the $[K(18\text{-c-}6)]^{1+}$ cation has a methyl group of a Me_3Si unit on one side and a methylene of a $(SiMe_2CH_2)$ moiety on the other side. There is precedence in the structural chemistry of

https://doi.org/10.1021/acs.inorgchem.3c00689
Inorg. Chem. 2023, 62, 5854−5862

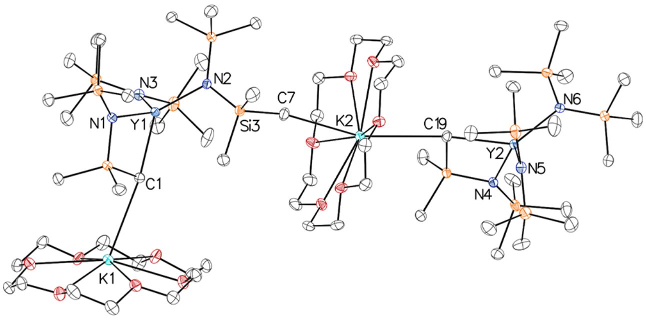

Figure 9. The molecular structure of the extended structure of $\{[K(18\text{-}c\text{-}6)]\{(R_2N)_2Y[N(SiMe_3)(SiMe_2CH_2)\text{-}\kappa C,\kappa N]\}\}_n$, **8-Y**, with thermal ellipsoids drawn at the 50% probability level. For clarity, hydrogen atoms are not shown.

the $[K(18\text{-}c\text{-}6)]^{1+}$ cation, showing that it can form extended structures with silylmethyl groups oriented toward the potassium.[62−65] In the (2,2,6,6-tetramethylpiperidin-1-yl)oxyl complex, $\{[(18\text{-}c\text{-}6)K][(\mu\text{-}Me_3Si)(Me_3Si)N]_2[Gd(NR_2)(\eta^1\text{-}ONC_5H_6Me_4)]\}_n$, trimethylsilyl groups are oriented to both sides of the $\{[(18\text{-}c\text{-}6)K]^{1+}$ cation.[66]

The $Y(NR_2)_3/KC_8$ reaction system also yielded a hydride product, $[K(18\text{-}c\text{-}6)][(R_2N)_3YH]$, **9-Y** (eq 11, Figure 10), which was a complex crystallized from the reduction of $Y(NR_2)_3$ with excess KC_8 in Et_2O in the presence of 18-c-6. The hydride ligand in **9-Y** is formally the "other" product of a reductive C−H bond cleavage that forms the $[N(SiMe_3)(SiMe_2CH_2)\text{-}\kappa C,\kappa N]^{2-}$ dianion. Formation of hydride byproducts in rare-earth reduction reactions has been observed before in the reduction of $[((^{Ad,Me}ArO)_3mes)Ln]$[73−75] and of $[((^{Ad,Me}ArO)_3mes)\text{-}U]$.[73,77] This yttrium hydride is unusual in that the hydride ligand is oriented toward the $[K(18\text{-}c\text{-}6)]^{1+}$ cation. A chelate-free dimeric version of this yttrium hydride, $(R_2N)_3Y[K(\mu_3\text{-}H)]_2Y(NR_2)_3$, has been previously reported from the hydrogenation of the reaction product of $Y(NR_2)_3$ with benzylpotassium.[78]

Crystallographic Details: Ln−O Structures. In four of the six structures containing Ln−O bonds derived from C−O bond cleavage reactions described here, the rare-earth metals are coordinated by three amide ligands and an anionic oxygen donor atom ligand and require countercations for charge balance: $[K(crypt)][(R_2N)_3Y(OCH_2CH_2OCH_3)]$, **1-Y**, $[K_2(18\text{-}c\text{-}6)_3]\text{-}\{[(R_2N)_3Lu]_2[(\mu\text{-}OCH_2CH_2O)]\}$, **3-Lu**, $[K(crypt)][(R_2N)_3Y\text{-}(OCH_2CH_2CH_2CH_3)]$, **4-Y**, and $[K(18\text{-}c\text{-}6)(OC_3H_6)]\text{-}[(R_2N)_3Ln(OCH_2CH_2CH_3)]$, **5-Ln**. These are analyzed as a group in Table 1. The remaining complexes, $[(R_2N)_2Y(\mu\text{-}OCH_2CH_2OMe\text{-}\kappa O,\kappa O')]_2$, **2-Y**, and $\{[(R_2N)_2]Y[\mu\text{-}O_2(C_{10}H_{20}O_4\text{-}\kappa O,\kappa O')K]\}_2$, **6-Y**, differ in that each contains two amides per rare-earth metal and no countercation since the overall complexes are neutral. These are compared in Table 2.

Complexes **1-Y**, **3-Lu**, **4-Y**, and **5-Ln** all have a distorted tetrahedral coordination environment around the rare-earth metal formed by the three amide ligands and one O-bound ligand. As shown in Table 1, the Ln−N distances fall in the narrow range of 2.25−2.30 Å since the structures are similar, and the metals have similar ionic radii. The Ln−O distances and Ln−O−C angles are also similar as are the N−Ln−N and N−Ln−O angles. In **5-Ho** and **5-Er**, both show an interaction between a methyl group of the $SiMe_3$ moiety and the potassium atom with closest C−K distances of 3.280(3) Å and 3.285(3) Å, for Ho and Er, respectively.

Complex $[(R_2N)_2Y(\mu\text{-}OCH_2CH_2OMe\text{-}\kappa O,\kappa O')]_2$, **2-Y**, has Ln−O bond distances that are longer compared to **1-Y**, **3-Lu**, **4-Y**, and **5-Ln** because the anionic oxygen donor atom in the methoxyethoxide ligands is bridging with Y(1)−O(1)′ 2.253(1) Å and Y(1)−O(1) 2.311(1) Å distances and the chelate oxygen is a neutral ether donor with a Y(1)−O(2) 2.369(1) Å distance.

Complex **6-Y**, $\{[(R_2N)_2]Y[\mu\text{-}O_2(C_{10}H_{20}O_4\text{-}\kappa O,\kappa O')K]\}_2$, also has two amide ligands per yttrium like **2-Y**, and has similar Y−N distances although the coordination number is four in **6-Y** and five in **2-Y**. Each oxygen of the chelating bis(alkoxide) ligand derived from 18-c-6 bridges Y and K with Y−O bond distances of 2.085(1) and 2.104(1) Å, respectively.

The $[K(crypt)]\{(R_2N)_2Y[N(SiMe_3)(SiMe_2CH_2)\text{-}\kappa C,\kappa N]\})$, **7-Y**, complexes have two conventional $(R_2N)^{1-}$ amide ligands per metal like **2-Y** and **6-Y**, along with another amide that has been metalated to form a dianion. All the Ln−N distances are in the range of 2.24−2.30 Å similar to those above. The Ln−C distances are longer at 2.44−2.70 Å.

The $(18\text{-}c\text{-}6)K(\mu\text{-}H)Y(R_2N)_3Y$ complex, **9-Y**, is a tris-amide complex with an unusual hydride ligand oriented toward the potassium in the 18-c-6 ligand. The Y−N distances fall within the range of the other complexes in this study, which demonstrates that these bond lengths are rather uniform across a variety of complexes. The metal hydride distances cannot be determined with great accuracy, but it appears that hydride is significantly closer to yttrium (2.18(4) Å) than potassium (2.61(4) Å). Hence, **9-Y** constitutes yet another example of how the $[K(18\text{-}c\text{-}6)]^{1+}$ cation orients in crystals to add electron density around potassium.

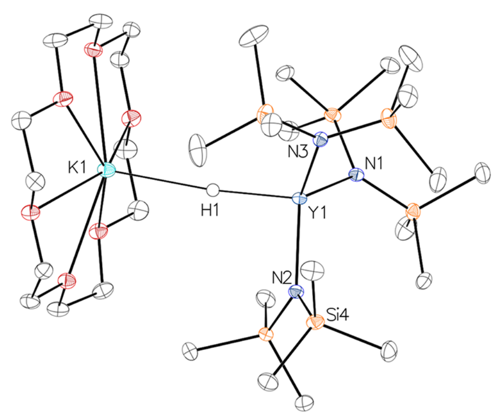

Figure 10. The molecular structure of $[K(18\text{-}c\text{-}6)][(R_2N)_3YH]$, **9-Y**, with atomic displacement parameters drawn at the 30% probability level. All hydrogen atoms are excluded for clarity except the hydride ligand.

■ CONCLUSIONS

The high reactivity of the $Ln(NR_2)_3/KC_8$ reduction system is demonstrated by X-ray crystal structures of six different types of C−O bond cleavage products that result from decomposition of DME, THF, oxetane, and 18-c-6. When other substrates are absent and if the low temperatures needed to isolate the Ln(II) complexes, $[Ln(NR_2)_3]^{1-}$, are not maintained, the systems will clearly decompose solvents. As shown here, a variety of alkoxide products result from these reactions including $(OCH_2CH_2OCH_3)^{1-}$, $(OCH_2CH_2O)^{2-}$, $(OCH_2CH_2CH_2CH_3)^{1-}$, $(OCH_2CH_2CH_3)^{1-}$, and $[O_2(C_{10}H_{20}O_4)]^{2-}$. Although Et_2O is not attacked by this system, decomposition can occur in this solvent via C−H bond activation that generates complexes of the $[N(SiMe_3)\text{-}$

https://doi.org/10.1021/acs.inorgchem.3c00689
Inorg. Chem. 2023, 62, 5854−5862

Table 1. Selected Bond Distances (Å) and Angles (°) for [K(Crypt)][$(R_2N)_3Y(OCH_2CH_2OCH_3)$], 1-Y, [$K_2$(18-c-6)$_3$]{[$(R_2N)_3Lu]_2[(\mu$-$OCH_2CH_2O)$]}, 3-Lu, [K(Crypt)][$(R_2N)_3Y(OCH_2CH_2CH_2$-$CH_3)$], 4-Y, and [K(18-c-6)($OC_3H_6$)][$(R_2N)_3Ln(OCH_2CH_2CH_3)$], 5-Ln (Ln = Ho, Er)

	Ln−O	Ln−N	C−O−Ln	N−Ln−N	N−Ln−O
1-Y	2.115(4)	2.25(1)−2.30(1)	159.0(5)	114.7(1)−117.0(5)	102.0(1)−104.6(1)
3-Lu	2.113(3)	2.234(2)−2.247(2)	159.2(4)	113.02(8)−117.08(8)	101.21(10)−106.10(10)
4-Y	2.038(4)	2.288(4)−2.298(4)	161.4(5)	113.39(14)−116.04(13)	101.85(17)−103.00(14)
5-Ho	2.045(2)	2.280(2)−2.293(2)	165.2(2)	112.89(8)−116.33(8)	103.27(9)−103.91(9)
5-Er	2.036(2)	2.270(2)−2.288(2)	164.9(2)	112.77(7)−116.09(7)	103.69(7)−104.27(7)

Table 2. Selected Bond Distances (Å) and Angles (°) for [$(R_2N)_2Y(\mu$-OCH_2CH_2OMe-$\kappa O,\kappa O')]_2$, 2-Y, and {[$(R_2N)_2$]Y[μ-$O_2(C_{10}H_{20}O_4$-$\kappa O,\kappa O')$K]}$_2$, 6-Y

	Ln−O	Ln−N	C−O−Ln	N−Ln−N	N−Ln−O
2-Y	2.253(2)−2.370 (2)	2.239(2), 2.283(2)	113.99(11)−132.50(12)	114.73(6)	98.26(5)−127.05(5)
6-Y	2.085(2), 2.104(2)	2.273(2), 2.285(2)	151.36(12), 142.82(12)	122.10(5)	104.36(5)−116.72(5)

$(SiMe_2CH_2)$-$\kappa C,\kappa N]^{2-}$ cyclometalate dianion as well as a hydride complex. Formation of the cyclometalate is common in $Ln(NR_2)_3$ reactions, and NMR studies of the C−O cleavage reactions show that it is generally formed in higher yield than the C−O cleavage products, although the cleavage products crystallize more readily.

■ ASSOCIATED CONTENT

Supporting Information

The Supporting Information is available free of charge at https://pubs.acs.org/doi/10.1021/acs.inorgchem.3c00689.

Experimental details and crystallographic details (PDF)

Accession Codes

CCDC entries 2215326−2215337 contain the supplementary crystallographic data for this paper. These data can be obtained free of charge via www.ccdc.cam.ac.uk/data_request/cif, or by emailing data_request@ccdc.cam.ac.uk, or by contacting The Cambridge Crystallographic Data Centre, 12 Union Road, Cambridge CB2 1EZ, UK; fax: +44 1223 336033.

■ AUTHOR INFORMATION

Corresponding Author

William J. Evans − *Department of Chemistry, University of California, Irvine, California 92697-2025, United States;* orcid.org/0000-0002-0651-418X; Email: wevans@uci.edu

Authors

Amanda B. Chung − *Department of Chemistry, University of California, Irvine, California 92697-2025, United States;* orcid.org/0000-0001-8943-0303

Cary R. Stennett − *Department of Chemistry, University of California, Irvine, California 92697-2025, United States;* orcid.org/0000-0002-2727-5747

William N. G. Moore − *Department of Chemistry, University of California, Irvine, California 92697-2025, United States;* orcid.org/0000-0001-5074-9341

Ming Fang − *Department of Chemistry, University of California, Irvine, California 92697-2025, United States*

Joseph W. Ziller − *Department of Chemistry, University of California, Irvine, California 92697-2025, United States;* orcid.org/0000-0001-7404-950X

Complete contact information is available at: https://pubs.acs.org/10.1021/acs.inorgchem.3c00689

Author Contributions

[#]A.B.C. and C.R.S. contributed equally to this work.

Notes

The authors declare no competing financial interest.

■ ACKNOWLEDGMENTS

We thank the U.S. National Science Foundation for the support of this research under CHE-2154255.

■ REFERENCES

(1) Gun'ko, Y. K.; Hitchcock, P. B.; Lappert, M. F. Activation of a C−O Bond by Reaction of a Tris(Cyclopentadienyl)Lanthanide Complex with an Alkali Metal in Dimethoxyethane (DME); Crystal Structures of [Nd{η-$C_5H_3(SiMe_3)_2$-1,3}$_2(\mu$-$OMe)_2$Li(DME)] and [{Ce(η-$C_5H_3{}^tBu_2$-1,3)$_2(\mu$-$OMe)_2$]. *J. Organomet. Chem.* **1995**, *499*, 213−219.

(2) Cassani, M. C.; Gun'ko, Y. K.; Hitchcock, P. B.; Lappert, M. F. The First Metal Complexes Containing the 1,4-Cyclohexa-2,5-Dienyl Ligand (Benzene 1,4-Dianion); Synthesis and Structures of [K(18-Crown-6)][Ln{η^5-$C_5H_3(SiMe_3)_2$-1,3}$_2(C_6H_6)$](Ln = La, Ce). *Chem. Commun.* **1996**, *16*, 1987−1988.

(3) Cristina Cassani, M.; Lappert, M. F.; Laschi, F. First Identification by EPR Spectra of Lanthanum(II) Organometallic Intermediates (and $E_{1/2}$ for $La^{3+} \rightarrow La^{2+}$) in the C−O Bond Activation of Dimethoxyethane. *Chem. Commun.* **1997**, *16*, 1563−1564.

(4) Cassani, M. C.; Duncalf, D. J.; Lappert, M. F. The First Example of a Crystalline Subvalent Organolanthanum Complex: [K([18]Crown-6)-(η^2-$C_6H_6)_2$][$(LaCp^{tt}{}_2)_2(\mu$-η^6:η^6-$C_6H_6)$]·$2C_6H_6$ (Cp^{tt} = η^5-$C_5H_3Bu^t{}_2$-1,3). *J. Am. Chem. Soc.* **1998**, *120*, 12958−12959.

(5) Cassani, M. C.; Gun'ko, Y. K.; Hitchcock, P. B.; Lappert, M. F.; Laschi, F. Synthesis and Characterization of Organolanthanidocene-(III) (Ln = La, Ce, Pr, Nd) Complexes Containing the 1,4-Cyclohexa-2,5-Dienyl Ligand (Benzene 1,4-Dianion): Structures of [K([18]-Crown-6)][Ln{η^5-$C_5H_3(SiMe_3)_2$-1,3}$_2(C_6H_6)$] [Cp″ = η^5-$C_5H_3(SiMe_3)_2$-1,3. *Organometallics* **1999**, *18*, 5539−5547.

(6) Gun'ko, Y. K.; Hitchcock, P. B.; Lappert, M. F. Nonclassical Organolanthanoid Metal Chemistry: [K([18]-Crown-6)(η^2-$PhMe)_2$]X (X = [$(LnCp^t{}_3)_2(\mu$-H)], [$(LnCp''{}_2)_2(\mu$-η^6:η^6-PhMe)]) from [$LnCp^x{}_3$], K, and [18]-Crown-6 in Toluene (Ln = La, Ce; Cp^t = η^5-$C_5H_4SiMe_2Bu^t$; Cp″ = η^5-$C_5H_3(SiMe_3)_2$-1,3). *Organometallics* **2000**, *19*, 2832−2834.

(7) Cristina Cassani, M.; Gun'ko, Y. K.; Hitchcock, P. B.; Hulkes, A. G.; Khvostov, A. V.; Lappert, M. F.; Protchenko, A. V. Aspects of Non-Classical Organolanthanide Chemistry. *J. Organomet. Chem.* **2002**, *647*, 71−83.

(8) Hitchcock, P. B.; Lappert, M. F.; Maron, L.; Protchenko, A. V. Lanthanum Does Form Stable Molecular Compounds in the +2 Oxidation State. *Angew. Chem., Int. Ed.* **2008**, *47*, 1488−1491.

(9) Coles, M. P.; Hitchcock, P. B.; Lappert, M. F.; Protchenko, A. V. Syntheses and Structures of the Crystalline, Highly Crowded 1,3-Bis(Trimethylsilyl)Cyclopentadienyls [MCp''_3] (M = Y, Er, Yb), [$PbCp''_2$], [{$YCp''_2(\mu$-OH)}$_2$], [$(ScCp''_2)_2(\mu$-η^2:η^2-C_2H_4)], [$YbCp''_2Cl(\mu$-Cl)K(18-Crown-6)], and [{KCp''}$_\infty$]. *Organometallics* **2012**, *31*, 2682−2690.

(10) Tilley, T. D.; Boncella, J. M.; Berg, D. J.; Burns, C. J.; Andersen, R. A.; Lawless, G. A.; Edelman, M. A.; Lappert, M. F. Bis[Bis-(Trimethylsilyl)Amido]Bis(Diethyl Ether)Ytterbium and (Diethyl Ether)Bis(η^5-Pentamethylcyclopentadienyl)Ytterbium. *Inorg. Synth.* **1990**, *27*, 146−150.

(11) Woen, D. H.; Evans, W. J. Chapter 293 - Expanding the +2 Oxidation State of the Rare-Earth Metals, Uranium, and Thorium in Molecular Complexes. *Handbook on the physics and Chemistry of Rare Earths*. 2016, *50*, 337−394, DOI: 10.1016/bs.hpcre.2016.08.002.

(12) Corbett, J. D. Reduced Halides of the Rare Earth Elements. *Rev. Chim. Miner.* **1973**, *10*, 239−257.

(13) Nief, F. Chapter 246 - Molecular Chemistry of the Rare-Earth Elements in Uncommon Low-Valent States. *Handbook on the Physics and Chemistry of Rare Earths*. 2010, *40*, 241−300.

(14) Bochkarev, M. N. Molecular Compounds of "New" Divalent Lanthanides. *Coord. Chem. Rev.* **2004**, *248*, 835−851.

(15) Morss, L. R. Thermochemical Properties of Yttrium, Lanthanum, and the Lanthanide Elements and Ions. *Chem. Rev.* **1976**, *76*, 827−841.

(16) MacDonald, M. R.; Bates, J. E.; Ziller, J. W.; Furche, F.; Evans, W. J. Completing the Series of +2 Ions for the Lanthanide Elements: Synthesis of Molecular Complexes of Pr^{2+}, Gd^{2+}, Tb^{2+}, and Lu^{2+}. *J. Am. Chem. Soc.* **2013**, *135*, 9857−9868.

(17) Palumbo, C. T.; Darago, L. E.; Windorff, C. J.; Ziller, J. W.; Evans, W. J. Trimethylsilyl versus Bis(Trimethylsilyl) Substitution in Tris-(Cyclopentadienyl) Complexes of La, Ce, and Pr: Comparison of Structure, Magnetic Properties, and Reactivity. *Organometallics* **2018**, *37*, 900−905.

(18) Ryan, A. J.; Ziller, J. W.; Evans, W. J. The Importance of the Counter-Cation in Reductive Rare-Earth Metal Chemistry: 18-Crown-6 Instead of 2,2,2-Cryptand Allows Isolation of [$Y^{II}(NR_2)_3$]$^{1-}$ and Ynediolate and Enediolate Complexes from CO Reactions. *Chem. Sci.* **2020**, *11*, 2006−2014.

(19) Ryan, A. J.; Balasubramani, S. G.; Ziller, J. W.; Furche, F.; Evans, W. J. Formation of the End-on Bound Lanthanide Dinitrogen Complexes [$(R_2N)_3Ln{-}N{=}N{-}Ln(NR_2)_3$]$^{2-}$ from Divalent [$(R_2N)_3Ln$]$^{1-}$ Salts (R = $SiMe_3$). *J. Am. Chem. Soc.* **2020**, *142*, 9302−9313.

(20) Woen, D. H.; Chen, G. P.; Ziller, J. W.; Boyle, T. J.; Furche, F.; Evans, W. J. End-On Bridging Dinitrogen Complex of Scandium. *J. Am. Chem. Soc.* **2017**, *139*, 14861−14864.

(21) Woen, D. H.; Huh, D. N.; Ziller, J. W.; Evans, W. J. Reactivity of Ln(II) Complexes Supported by $(C_5H_4Me)^{1-}$ Ligands with THF and $PhSiH_3$: Isolation of Ring-Opened, Bridging Alkoxyalkyl, Hydride, and Silyl Products. *Organometallics* **2018**, *37*, 3055−3063.

(22) Niemeyer, M. Reactions of Hypersilyl Potassium with Rare-Earth Metal Bis(Trimethylsilylamides): Addition versus Peripheral Deprotonation. *Inorg. Chem.* **2006**, *45*, 9085−9095.

(23) Fang, M.; Bates, J. E.; Lorenz, S. E.; Lee, D. S.; Rego, D. B.; Ziller, J. W.; Furche, F.; Evans, W. J. $(N_2)^{3-}$ Radical Chemistry via Trivalent Lanthanide Salt/Alkali Metal Reduction of Dinitrogen: New Syntheses and Examples of $(N_2)^{2-}$ and $(N_2)^{3-}$ Complexes and Density Functional Theory Comparisons of Closed Shell Sc^{3+}, Y^{3+}, and Lu^{3+} versus $4f^9$ Dy^{3+}. *Inorg. Chem.* **2011**, *50*, 1459−1469.

(24) Simpson, S. J.; Turner, H. W.; Andersen, R. A. Preparation and Hydrogen-Deuterium Exchange of Alkyl and Hydride Bis-(Trimethylsilyl)Amido Derivatives of the Actinide Elements. *Inorg. Chem.* **1981**, *20*, 2991−2995.

(25) Karl, M.; Harms, K.; Seybert, G.; Massa, W.; Fau, S.; Frenking, G.; Dehnicke, K. Die Deprotonierung Silylierter Amido-Komplexe von Seltenerdelementen. *Z. Anorg. Allg. Chem.* **1999**, *625*, 2055−2063.

(26) Deacon, G. B.; Forsyth, C. M. Linkage Isomerism and C−H Activation in an Ytterbium(II) Tetraphenylborate. *Chem. Commun.* **2002**, *21*, 2522−2523.

(27) Wang, J.; Gardiner, M. G. C−H Activation (γ-Deprotonation) of a Sm(III) Bis(Trimethylsilyl)Amide Complex via Macrocyclic Stabilisation of the Sodium Counter Ion. *Chem. Commun.* **2005**, *12*, 1589−1591.

(28) Deacon, G. B.; Forsyth, C. M.; Junk, P. C.; Wang, J. Reduction of Carbodiimides by Samarium(II) Bis(trimethylsilyl)amides - Formation of Oxalamidinates and Amidinates through C−C Coupling or C−H Activation. *Inorg. Chem.* **2007**, *46*, 10022−10030.

(29) Jenkins, T. F.; Bekoe, S.; Ziller, J. W.; Furche, F.; Evans, W. J. Synthesis of a Heteroleptic Pentamethylcyclopentadienyl Yttrium(II) Complex, [K(2.2.2-Cryptand)]{$(C_5Me_5)_2Y^{II}[N(SiMe_3)_2]$}, and Its C−H Bond Activated Y(III) Derivative. *Organometallics* **2021**, *40*, 3917−3925.

(30) Wedal, J. C.; Ziller, J. W.; Furche, F.; Evans, W. J. Synthesis and Reduction of Heteroleptic Bis(Cyclopentadienyl) Uranium(III) Complexes. *Inorg. Chem.* **2022**, *61*, 7365−7376.

(31) Jaroschik, F.; Nief, F.; Le Goff, X.-F.; Ricard, L. Isolation of Stable Organodysprosium(II) Complexes by Chemical Reduction of Dysprosium(III) Precursors. *Organometallics* **2007**, *26*, 1123−1125.

(32) Corbey, J. F.; Woen, D. H.; Palumbo, C. T.; Fieser, M. E.; Ziller, J. W.; Furche, F.; Evans, W. J. Ligand Effects in the Synthesis of Ln^{2+} Complexes by Reduction of Tris(Cyclopentadienyl) Precursors Including C−H Bond Activation of an Indenyl Anion. *Organometallics* **2015**, *34*, 3909−3921.

(33) Dormond, A.; El Bouadili, A. A.; Moïse, C. Reactivity of the Actinoid−Carbon σ Bond: Reaction of [$(Me_3Si)_2N]_2MCH_2Si$-$(Me)_2NSiMe_3$ with Acidic Hydrogen, Ready C−H Activation. *J. Chem. Soc., Chem. Commun.* **1985**, *13*, 914−916.

(34) Trnka, T. M.; Bonanno, J. B.; Bridgewater, B. M.; Parkin, G. Bis(Permethylindenyl) Complexes of Thorium: Synthesis, Structure, and Reactivity. *Organometallics* **2001**, *20*, 3255−3264.

(35) Fortier, S.; Wu, G.; Hayton, T. W. Synthesis of a Nitrido-Substituted Analogue of the Uranyl Ion, $[N{\equiv}U{\equiv}O]^+$. *J. Am. Chem. Soc.* **2010**, *132*, 6888−6889.

(36) Fortier, S.; Kaltsoyannis, N.; Wu, G.; Hayton, T. W. Probing the Reactivity and Electronic Structure of a Uranium(V) Terminal Oxo Complex. *J. Am. Chem. Soc.* **2011**, *133*, 14224−14227.

(37) Hervé, A.; Bouzidi, Y.; Berthet, J.-C.; Belkhiri, L.; Thuéry, P.; Boucekkine, A.; Ephritikhine, M. U^{III}−CN versus U^{IV}−NC Coordination in Tris(Silylamide) Complexes. *Inorg. Chem.* **2015**, *54*, 2474−2490.

(38) Rookes, T. M.; Wildman, E. P.; Balázs, G.; Gardner, B. M.; Wooles, A. J.; Gregson, M.; Tuna, F.; Scheer, M.; Liddle, S. T. Actinide−Pnictide (An−Pn) Bonds Spanning Non-Metal, Metalloid, and Metal Combinations (An=U, Th; Pn=P, As, Sb, Bi). *Angew. Chem., Int. Ed.* **2018**, *57*, 1332−1336.

(39) Staun, S. L.; Sergentu, D.-C.; Wu, G.; Autschbach, J.; Hayton, T. W. Use of ^{15}N NMR Spectroscopy to Probe Covalency in a Thorium Nitride. *Chem. Sci.* **2019**, *10*, 6431−6436.

(40) Wedal, J. C.; Bekoe, S.; Ziller, J. W.; Furche, F.; Evans, W. J. C−H Bond Activation via U(II) in the Reduction of Heteroleptic Bis(Trimethylsilyl)Amide U(III) Complexes. *Organometallics* **2020**, *39*, 3425−3432.

(41) Evans, W. J.; Lee, D. S.; Rego, D. B.; Perotti, J. M.; Kozimor, S. A.; Moore, E. K.; Ziller, J. W. Expanding Dinitrogen Reduction Chemistry to Trivalent Lanthanides via the LnZ_3/Alkali Metal Reduction System: Evaluation of the Generality of Forming $Ln_2(\mu$-η^2:η^2-$N_2)$ Complexes via LnZ_3/K. *J. Am. Chem. Soc.* **2004**, *126*, 14574−14582.

(42) Shannon, R. D. Revised Effective Ionic Radii and Systematic Studies of Interatomic Distances in Halides and Chalcogenides. *Acta Crystallogr. Sect. A* **1976**, *32*, 751−767.

(43) Luo, Y.; Feng, X. Synthesis and Crystal Structure of [$Y(C_5Me_4SiMe_3)${μ-$O(CH_2)_3CH_3$}{$N(SiHMe_2)_2$}]$_2$. *J. Rare Earths* **2011**, *29*, 24−27.

(44) Spinney, H. A.; Clough, C. R.; Cummins, C. C. The Titanium Tris-Anilide Cation $[Ti(N[^tBu]Ar)_3]^+$ Stabilized as Its Perfluoro-Tetra-Phenylborate Salt: Structural Characterization and Synthesis in Connection with Redox Activity of 4,4′-Bipyridine Dititanium Complexes. *Dalton Trans.* **2015**, *44*, 6784−6796.

https://doi.org/10.1021/acs.inorgchem.3c00689
Inorg. Chem. 2023, 62, 5854−5862

(45) Liu, D.; Wang, Y.; Chan, H.-S.; Tang, Y.; Xie, Z. Synthesis, Structure, and Reactivity of Group 4 Metallacarboranes Bearing the Ligand $[Me_2C(C_9H_6)(C_2B_9H_{10})]^{3-}$. *Organometallics* **2008**, *27*, 5295–5302.
(46) Mukherjee, D.; Osseili, H.; Truong, K.-N.; Spaniol, T. P.; Okuda, J. Ring-Opening of Cyclic Ethers by Aluminum Hydridotriphenylborate. *Chem. Commun.* **2017**, *53*, 3493–3496.
(47) Fryzuk, M. D.; Clentsmith, G. K. B.; Rettig, S. J. Coordination Behaviour of $LiBEt_4$ towards $(\eta^5\text{-}C_5H_5)_2ReH$, $(\eta^5\text{-}C_5H_5)_2WH_2$ and $(\eta^5\text{-}C_5H_5)_2TaH_3$. Solid State Structure of $[(\eta^5\text{-}C_5H_5)_2TaH \cdot AlH_2(OCH_2CH_2CH_2CH_3)]_2$. *Inorg. Chim. Acta* **1997**, *259*, 51–59.
(48) Boncella, J. M.; Cajigal, M. L.; Gamble, A. S.; Abboud, K. A. Synthesis and Crystal Structures of Hydridotris(3,5-Dimethylpyrazolyl) Borate Tantalum(V)(=N-2,6-$Pr_2C_6H_3$)(X)Cl (X = Cl, Bu^{n}O). *Polyhedron* **1996**, *15*, 2071–2078.
(49) Cheng, J.; Wang, H.; Nishiura, M.; Hou, Z. Binuclear Rare-Earth Polyhydride Complexes Bearing Both Terminal and Bridging Hydride Ligands. *Chem. Sci.* **2012**, *3*, 2230–2233.
(50) Bonnet, F.; Da Costa Violante, C.; Roussel, P.; Mortreux, A.; Visseaux, M. Unprecedented Dual Behaviour of a Half-Sandwich Scandium-Based Initiator for Both Highly Selective Isoprene and Styrene Polymerisation. *Chem. Commun.* **2009**, *23*, 3380–3382.
(51) Deelman, B.-J.; Booij, M.; Meetsma, A.; Teuben, J. H.; Kooijman, H.; Spek, A. L. Activation of Ethers and Sulfides by Organolanthanide Hydrides. Molecular Structures of $(Cp^*{}_2Y)_2(\mu\text{-}OCH_2CH_2O)(THF)_2$ and $(Cp^*{}_2Ce)_2(\mu\text{-}O)(THF)_2$. *Organometallics* **1995**, *14*, 2306–2317.
(52) Zhu, H.; Chen, E. Y.-X. Tripodal Amido Boron and Aluminum Complexes. *Inorg. Chem.* **2007**, *46*, 1481–1487.
(53) Stanetty, P.; Koller, H.; Mihovilovic, M. Directed Ortho Lithiation of Phenylcarbamic Acid 1,1-Dimethylethyl Ester (N-BOC-Aniline). Revision and Improvements. *J. Org. Chem.* **1992**, *57*, 6833–6837.
(54) Bates, R. B.; Kroposki, L. M.; Potter, D. E. Cycloreversions of Anions from Tetrahydrofurans. Convenient Synthesis of Lithium Enolates of Aldehydes. *J. Org. Chem.* **1972**, *37*, 560–562.
(55) Maercker, A. Ether Cleavage with Organo-Alkali-Metal Compounds and Alkali Metals. *Angew. Chem. Int. Ed.* **1987**, *26*, 972–989.
(56) Schwamm, R. J.; Coles, M. P.; Hill, M. S.; Mahon, M. F.; McMullin, C. L.; Rajabi, N. A.; Wilson, A. S. S. A Stable Calcium Alumanyl. *Angew. Chem., Int. Ed.* **2020**, *59*, 3928–3932.
(57) Clayden, J.; Yasin, S. A. Pathways for Decomposition of THF by Organolithiums: The Role of HMPA. *New J. Chem.* **2002**, *26*, 191–192.
(58) Mulvey, R. E.; Blair, V. L.; Clegg, W.; Kennedy, A. R.; Klett, J.; Russo, L. Cleave and Capture Chemistry Illustrated through Bimetallic-Induced Fragmentation of Tetrahydrofuran. *Nature Chem.* **2010**, *2*, 588–591.
(59) Guan, J.; Dubé, T.; Gambarotta, S.; Yap, G. P. A. Dinitrogen Labile Coordination versus Four-Electron Reduction, THF Cleavage, and Fragmentation Promoted by a (Calix-Tetrapyrrole)Sm(II) Complex. *Organometallics* **2000**, *19*, 4820–4827.
(60) Korobkov, I.; Gambarotta, S.; Yap, G. P. A. Highly Reactive Uranium(III) Polypyrrolide Complexes: Intramolecular C–H Bond Activation, Ligand Isomerization, and Solvent Deoxygenation and Fragmentation. *Organometallics* **2001**, *20*, 2552–2559.
(61) Anet, F. A. L.; O'Leary, D. J. H-D Coupling Constants and Deuterium Isotope Effects on the Proton Chemical Shifts in Partially Deuteriated Methanes. *Tetrahedron Lett.* **1989**, *30*, 2755–2758.
(62) Westerhausen, M.; Weinrich, S.; Schmid, B.; Schneiderbauer, S.; Suter, M.; Nöth, H.; Piotrowski, H. Synthese, Spektroskopische Charakterisierung Und Molekülstrukturen Ausgewählter Lewis-Basen-Addukte Der Alkalimetall-Tri(Tert-Butyl)Silylphosphanide. *Z. Anorg. Allg. Chem.* **2003**, *629*, 625–633.
(63) Likhar, P. R.; Zirngast, M.; Baumgartner, J.; Marschner, C. Preparation and Structural Characterisation of Methoxybis-(Trimethylsilyl)Silyl Potassium and Its Condensation Product. *Chem. Commun.* **2004**, *15*, 1764–1765.
(64) Zitz, R.; Hlina, J.; Arp, H.; Kinschel, D.; Marschner, C.; Baumgartner, J. Group 4 Metal and Lanthanide Complexes in the Oxidation State +3 with Tris(Trimethylsilyl)Silyl Ligands. *Inorg. Chem.* **2019**, *58*, 7107–7117.
(65) Evans, W. J.; Giarikos, D. G.; Workman, P. S.; Ziller, J. W. Utility of Anhydrous Neodymium Nitrate as a Precursor to Extended Organoneodymium Nitrate Networks. *Inorg. Chem.* **2004**, *43*, 5754–5760.
(66) Chung, A. B.; Ryan, A. J.; Fang, M.; Ziller, J. W.; Evans, W. J. Reductive Reactivity of the $4f^75d^1$ Gd(II) Ion in $\{Gd^{II}[N(SiMe_3)_2]_3\}^-$: Structural Characterization of Products of Coupling, Bond Cleavage, Insertion, and Radical Reactions. *Inorg. Chem.* **2021**, *60*, 15635–15645.
(67) Huh, D. N.; Kotyk, C. M.; Gembicky, M.; Rheingold, A. L.; Ziller, J. W.; Evans, W. J. Synthesis of Rare-Earth-Metal-in-Cryptand Dications, $[Ln(2.2.2\text{-}Cryptand)]^{2+}$, from Sm^{2+}, Eu^{2+}, and Yb^{2+} Silyl Metallocenes $(C_5H_4SiMe_3)_2Ln(THF)_2$. *Chem. Commun.* **2017**, *53*, 8664–8666.
(68) Fang, M.; Farnaby, J. H.; Ziller, J. W.; Bates, J. E.; Furche, F.; Evans, W. J. Isolation of $(CO)^{1-}$ and $(CO_2)^{1-}$ Radical Complexes of Rare Earths via $Ln(NR_2)_3$/K Reduction and $[K_2(18\text{-}Crown\text{-}6)_2]^{2+}$ Oligomerization. *J. Am. Chem. Soc.* **2012**, *134*, 6064–6067.
(69) McGeary, M. J.; Folting, K.; Streib, W. E.; Huffman, J. C.; Caulton, K. G. Oligomerization and Structural Variation of Alkali Metal Silyloxides. *Polyhedron* **1991**, *10*, 2699–2709.
(70) Petrosyants, S. P.; Ulyukhin, A. B. Stabilization of $[Sc(NCS)_6]^{3-}$ Anion by $[M(18C6)]^+$ Complexes in Solvation Systems. *Russ. J. Coord. Chem.* **2007**, *33*, 155–159.
(71) Fischer, P. J.; Yuen, P.; Young, V. G.; Ellis, J. E. Novel Alkoxo- and Aryloxotitanium Carbonyls. Structural Characterization of $[Ti(CO)_4(\mu\text{-}OPh)]_2{}^{2-}$ 1. *J. Am. Chem. Soc.* **1997**, *119*, 5980–5981.
(72) Chekhlov, A. N. Synthesis and Crystal Structure of Hexakis-(Isothiocyanato)Erbium(III) Thiocyanate Bis(18-Crown-6)-Dipotassium Bis[(18-Crown-6)Ethanolpotassium]. *Russ. J. Coord. Chem.* **2008**, *34*, 849–854.
(73) Fieser, M. E.; Palumbo, C. T.; La Pierre, H. S.; Halter, D. P.; Voora, V. K.; Ziller, J. W.; Furche, F.; Meyer, K.; Evans, W. J. Comparisons of Lanthanide/Actinide +2 Ions in a Tris(Aryloxide)-Arene Coordination Environment. *Chem. Sci.* **2017**, *8*, 7424–7433.
(74) Palumbo, C. T.; Halter, D. P.; Voora, V. K.; Chen, G. P.; Chan, A. K.; Fieser, M. E.; Ziller, J. W.; Hieringer, W.; Furche, F.; Meyer, K.; Evans, W. J. Metal versus Ligand Reduction in Ln^{3+} Complexes of a Mesitylene-Anchored Tris(Aryloxide) Ligand. *Inorg. Chem.* **2018**, *57*, 2823–2833.
(75) Palumbo, C. T.; Halter, D. P.; Voora, V. K.; Chen, G. P.; Ziller, J. W.; Gembicky, M.; Rheingold, A. L.; Furche, F.; Meyer, K.; Evans, W. J. Using Diamagnetic Yttrium and Lanthanum Complexes to Explore Ligand Reduction and C–H Bond Activation in a Tris(Aryloxide)-Mesitylene Ligand System. *Inorg. Chem.* **2018**, *57*, 12876–12884.
(76) Ryan, A. J.; Darago, L. E.; Balasubramani, S. G.; Chen, G. P.; Ziller, J. W.; Furche, F.; Long, J. R.; Evans, W. J. Synthesis, Structure, and Magnetism of Tris(Amide) $[Ln\{N(SiMe_3)_2\}_3]^{1-}$ Complexes of the Non-Traditional +2 Lanthanide Ions. *Chem. Eur. J.* **2018**, *24*, 7702–7709.
(77) La Pierre, H. S.; Kameo, H.; Halter, D. P.; Heinemann, F. W.; Meyer, K. Coordination and Redox Isomerization in the Reduction of a Uranium(III) Monoarene Complex. *Angew. Chem., Int. Ed.* **2014**, *53*, 7154–7157.
(78) Zhai, D.-D.; Du, H.-Z.; Zhang, X.-Y.; Liu, Y.-F.; Guan, B.-T. Potassium Yttrium Ate Complexes: Synergistic Effect Enabled Reversible H_2 Activation and Catalytic Hydrogenation. *ACS Catal.* **2019**, *9*, 8766–8771.

https://doi.org/10.1021/acs.inorgchem.3c00689
Inorg. Chem. 2023, 62, 5854–5862